

The Evolution of Galaxies by MOND

Ding-Yu Chung*

In this paper, MOND (modified Newtonian dynamics) is derived from incompatible dark matter (IDM). The origin of MOND is the incompatibility between dark matter and baryonic matter. The cosmic evolution generates six mass dimensional particle matters from 5D to 10D and one 4D-particle matter, corresponding to dark matter and baryonic matter with the mass ratio of 6/1 as observed. Due to the structural difference, baryonic matter and dark matter are incompatible to each other as oil droplet and water in emulsion. In the interfacial zone between dark matter and baryonic matter, this incompatibility generates the modification of Newtonian dynamics to keep dark matter and baryonic matter apart. The five periods of baryonic structure development in the order of increasing incompatibility are the free baryonic matter, the baryonic droplet, the galaxy, the cluster, and the supercluster periods. The transition to the baryonic droplet generates density perturbation in the CMB. In the galaxy period, the first-generation galaxies include elliptical, normal spiral, barred spiral, irregular, and dwarf spheroidal galaxies. In the cluster period, the second-generation galaxies include modified giant ellipticals, cD, evolved S0, dwarf elliptical, BCD, and tidal dwarf galaxies. The whole observable expanding universe behaves as one unit of emulsion with increasing incompatibility between dark matter and baryonic matter. The origin of the mixture of 4D to 10D particles involves cosmology based on superstring.

Introduction

Two possible explanations for the discrepancies between the Newtonian dynamical mass and the directly observable mass in large astronomical systems are dark matter as unseen matter and MOND (modified Newtonian dynamics) [1]. In this paper, both explanations are combined into one explanation. The origin of MOND is the incompatibility between dark matter and baryonic matter. The cosmic evolution generates six mass dimensional particle matters from 5D to 10D and one 4D-particle matter, corresponding to dark matter and baryonic matter with the mass ratio of 6/1 as observed. Due to the structural difference, baryonic matter and dark matter are incompatible to each other as oil and water in emulsion. In the interfacial zone between dark matter and baryonic matter, this incompatibility generates the modification of Newtonian dynamics to keep dark matter and baryonic matter apart. Outside of this interfacial zone, Newtonian dynamics is normal. The incompatibility between dark matter and baryonic matter results in the “Milky Universe”, which explains the evolution of galaxies in details.

The origin of the mixture of 4D to 10D particles involves cosmology based on superstring. Section 1 describes variable space-time dimensions and variable mass dimensions. Section 2 describes the evolution of the expanding universe and objects-vacuums. The cosmic expansion mechanism and the two different modes of the cosmic

expansion are described in Section 3. The formation of inhomogenous structure in the observable universe based on the Milky Universe is described in Section 4. The evolution of galaxies is stated in Section 5.

1. *Variable Space-time Dimensions and Variable Mass Dimensions*

In VSL theory [2], the speed of light varies with its frequency, with higher speeds for higher frequencies and energies. Typically, the variable speed of light is assumed to be continuous. In this paper, the variable speed of light is quantized as follows.

$$c_D = c / \alpha^{D-4}, \quad (1)$$

where c_D is the variable quantized speed of light in space-time dimension, D , which is the Kaluza-Klein space-time dimension from 4 to 11. The speed of light in the four dimensional space-time is c , and α is the fine structure constant. Each space-time dimension has a specific speed of light. The speed of light increases with increasing space-time dimension number, D . In relativity, $E = M c^2$ modified by Eq. (1) is expressed as

$$E_D = M (c^2 / \alpha^{2(D-4)}) \quad (2a)$$

$$= (M / \alpha^{2(D-4)}) c^2 \quad (2b)$$

Eq. (2a) means that a particle in the D dimensional space-time has superluminal speed, c / α^{D-4} , that is higher than the normal speed of light. Eq. (2b) means that the same particle in the four-dimensional space-time with the normal speed of light acquires D dimensional mass $M/\alpha^{2(D-4)}$. D in Eq. (2a) is space-time dimension defining the variable speed of light. D from 4 to 11 in Eq. (2b) is “mass dimension” defining variable mass. If $D = 11$, Eq. (2a) shows a superluminal particle in eleven-dimensional space-time, while Eq. (2b) shows the space-time dimension of the same particle is four, and the mass dimension is eleven. Therefore, in relativity, quantized variable speed of light in terms of variable space-time dimension, D , brings about variable mass in terms of variable mass dimension, D .

Eq. (2) is possible, when vacuum energy determines the speed of light and space-time dimension. A particle in higher vacuum energy has lower rest mass than in lower vacuum energy, because the speed of light in higher vacuum energy is higher than in lower vacuum energy. In the four-dimensional space-time, the vacuum energy is zero with normal speed of light. The maximum space-time dimension is eleven, which has the minimum rest mass, $M_{0,11}$. The minimum space-time dimension is four, which has the maximum rest mass, the Planck mass (M_{PL}). The dimensional rest masses for space-time dimensions are

$$\begin{aligned} M_{0,D} &= M_{PL} \alpha^{2(D-4)} \\ &= M_{0,11} / \alpha^{2(11-D)} \end{aligned} \quad (3)$$

where D is space-time dimension from four to eleven.

In the same dimensional space-time and vacuum energy, a particle can transform (fractionalize or condense) into particles with different mass dimensions equal to or higher than its space-time dimension. For example, a particle with 4-dimensional space-time can have mass dimensions from 4 up to 11. The transformation is through “variable supersymmetry”. In the normal supersymmetry, the repeated application of the fermion-boson transformation transforms a boson (or fermion) from one point to the same boson (or fermion) at another point at the same mass. In the “variable supersymmetry”, the repeated application of the fermion-boson transformation transforms a boson from one point to the boson with different mass at another point at different mass dimension. The repeated variable supersymmetry transformation transforms boson B_D into fermion F_D and from fermion F_D to boson B_{D-1} is expressed as

$$M_{D,F} = M_{D,B} \alpha_{D,B}, \quad (4a)$$

$$M_{D-1,B} = M_{D,F} \alpha_{D,F}, \quad (4b)$$

where $M_{D,B}$ and $M_{D,F}$ are the masses for a boson and a fermion, respectively, D is mass dimension, and $\alpha_{D,B}$ or $\alpha_{D,F}$ is the fine structure constant, which is the ratio between the masses of a boson and its fermionic partner. Assuming $\alpha_{D,B} = \alpha_{D,F}$, the relation between the bosons in the adjacent dimensions, then, can be expressed as

$$M_{D-1,B} = M_{D,B} \alpha^2_D, \quad (4c)$$

which means that under variable supersymmetry, a particle moves and changes mass at the same time. Eq. (4c) is verified empirically in the Reference [3].

The maximum mass dimension is eleven, and the maximum mass is the Planck mass (M_{PL}). The lowest mass-dimensional mass is the four-mass-dimensional mass, M_4 . Assuming α is the same for all fermions and bosons,

$$\begin{aligned} M_D &= M_{PL} \alpha^{2(11-D)} \\ &= M_4 / \alpha^{2(D-4)} \end{aligned} \quad (5)$$

where D is mass dimension from four to eleven. As shown in the Reference [3], with one exception, α is same for all fermions and bosons, so Eq. (5) is approximately correct empirically.

In summary, variable space-time dimension (D) quantizes variable speed of light, resulting in variable mass in terms of variable mass dimension (D). Variable supersymmetry transforms (fractionalizes or condenses) variable mass. The decrease in quantized vacuum energy causes the increase in rest mass and the decrease in space-time dimension. A particle can move and fractionalize into the particles with the decrease in mass dimensions and masses. The combination of both variable space-time dimension and

variable mass dimension allows an $11D$ particle to move and fractionalize into $4D$ particles under decreasing vacuum energy, resulting in the cosmic expansion.

2. *From the Pre-universe to the Expanding Universe: Objects-Vacuums*

The evolution of our expanding universe involves four stages: the pre-universe, the pre-expanding universe, the mixed pre-expanding universe, and the expanding universe. Different stages of the evolution have different compositions of objects-vacuums. Objects have definite shapes, and vacuums have homogeneous spaces. Objects include string, membrane, particle, and particle-wave. Vacuums include object vacuum, single vacuum, inclusive vacuum, and exclusive vacuum. Object vacuum takes turn to coexist equally with object at the same location as in creation and annihilation of particle in vacuum. Single vacuum exists with an object at the same location or different locations in one object to one vacuum relation as in fermion space. Inclusive vacuum exists at the same location with multiple objects as in boson space. Exclusive vacuum excludes object at the same location as the space of traveling light in the sense that light is forced to travel by permanent exclusion of space by exclusive vacuum.

The pre-universe is essentially a homogeneous blank consisting of $10D$ superstring in equilibrium with vacuum at a non-zero vacuum energy and superluminal speed. The pre-universe is object vacuum-object, the equilibrium state between the vacuum and the pairs of ten-dimensional superstring and anti-superstring. The vacuum energy is equal to the non-zero energy of the superstring.

The condensation as the compactification of higher dimensions leads to the formation of a two space-time dimensional string and the empty space as single vacuum, each of which associates with one object. One object per vacuum is the definition of fermion.

The compact two space-time dimensional string has the Planck mass. This $2D$ string attaches to the $10D$ superstring to provide the eleventh dimension for an eleven-dimensional membrane as Fig. (1). The compact string has the Planck mass. The pre-universe is pre-quantum mechanics without uncertainty, so without uncertainty, the space-time of the $2D$ -string attaches to the space-time of the adjacent $10D$ -superstring precisely. This evolution from string to membrane is the reverse of M-theory that starts with $11D$ -membrane.

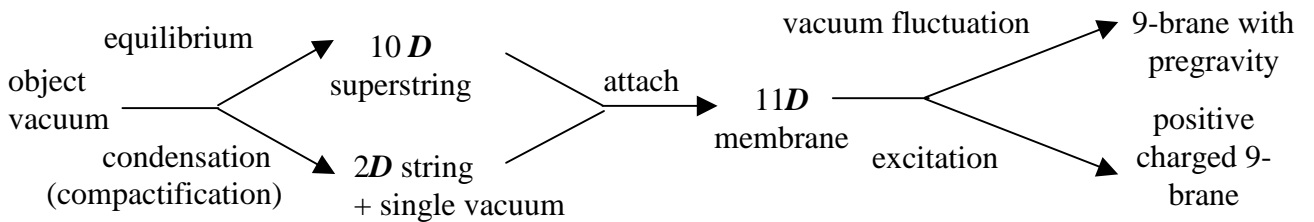


Fig. 1: the evolution of 9-brane in the pre-expanding universe

The attached string can undergo vacuum fluctuation and excitation. In terms of vacuum fluctuation, the non-zero vacuum energy causes the attached string to diffuse into single vacuum to become an infinite dimension. Subsequently, the attachment of the string in membrane provides AdS (anti-de Sitter space) for the diffused string to condense (compactify) again. When this diffusion-condensation overlaps with the diffusion-condensation from another membrane, "pregravity" (the predecessor of gravity) is formed. Pregravity is in inclusive vacuum that allows more than multiple objects per vacuum. Boson is defined as multiple objects per vacuum. This diffusion-condensation reproduces the Planck-infinite dimension in the Randall-Sundrum model [4] for gravity. The resulting structure is 9-brane (10D-brane) embedded in the eleven-dimensional bulk with pregravity. Since pregravity is active in an empty space, pregravity is a long-ranged force as Fig. 1 and Fig. 2.

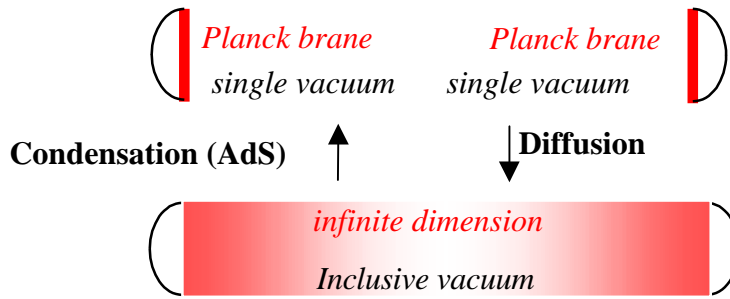


Fig. 2: pregravity as the Randall-Sundrum model

In terms of excitation, the attached string behaves as the 1D circle circling superstring in the 10D x 1D Kaluza-Klein structure. The quantized excitation of the circle brings about the quantized positive pre-charged force (the predecessor of electromagnetism) with the absorption and the emission of the massless particles in exchange with the massless particles from other membranes. Since the pre-charged force is active in empty space, the pre-charged force is a long-ranged force as Fig. 1 and Fig. 3.



Fig. 3: pre-charged force from excitation

The combination of the vacuum fluctuation and the excitation of the attached string results in the positive charged 9-brane embedded in the eleven-dimensional bulk with pregravity and positive pre-charged force (Fig. 1). At the same time, the ten-dimensional anti-superstring becomes negative charged 9-antibrane embedded in the eleven-dimensional bulk with anti-pregravity and negative pre-charged force.

The original force among strings in the pre-universe is the pre-strong force, the predecessor of the strong force. The force is resulted from the absorption and the emission of massless particles from strings. Since it transmits through object vacuum with non-zero energy, rather than an empty space, it is a short-ranged force through a non-zero energy medium. This pre-strong force remains as a short-ranged force among membranes.

The combination of the 9-brane and the 9-antibrane is the brane-antibrane unit. The structure of the brane-antibrane unit is determined by the evolutionary sequence of the three forces. In the normal evolutionary sequence, the pre-strong force exists first. Then, the emergence of the repulsive force between pregravity and anti-pregravity forces a brane and an antibrane to move away from each other. Subsequently, the pre-strong force connects the newly formed brane or the antibrane with previously formed branes or antibranes. Finally, the pre-charged force emerges. The space occupied by branes is opposite from the space occupied by antibranes, so branes and antibranes are chiral. This normal evolutionary sequence provides the chiral brane-antibrane unit where the chiral boundary positive charged 9-brane and the chiral boundary negative charged 9-antibrane embedded in the eleven-dimensional space-time are separated by chiral pregravity and chiral anti-pregravity as Fig. 4.

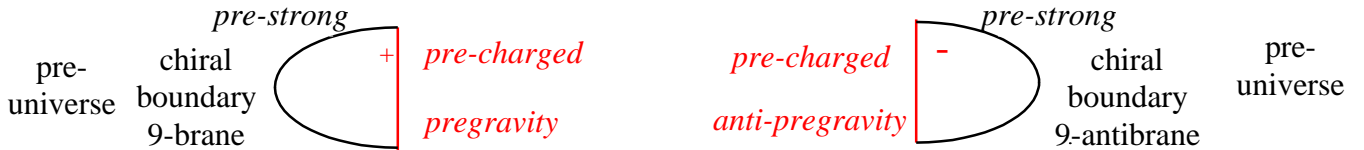


Fig. 4: the pre- expanding universe

The pre-expanding universe emerges with this chiral brane-antibrane unit as the predominant structure. All forces and membranes inside the pre-expanding universes are chiral. The pre-expanding universe continues to grow with the conversion of the pre-universe vacuum entering into the single vacuum in the middle of the pre-expanding universe. This two-brane structure of the pre-expanding universe also appears in the Horava-Witten eleven dimensional pregravity on a manifold with two ten-dimensional boundaries [5], the ekpyrotic universe boundary branes [6], and the brane-antibrane universe [7].

During the steady conversion from the pre-universe to the pre-expanding universe takes place, the total volume of the two universes remain constant. To maintain this constant volume, the attractive force (A) between the positive and negative pre-charged forces is equal to the sum of the repulsive force (R) between pregravity and anti-pregravity, and the special global short-ranged pre-strong force (C) connecting the pre-expanding universe and the pre-universe. $A = R + C$ is a non-localized global relation for the constant total volume of the universes. If $A > R + C$, the total volume is smaller, and if $A < R + C$, the total volume is larger.

There is a small amount of the abnormal evolutionary sequence in the pre-expanding universe. In the abnormal evolutionary sequence, the pre-strong force exists first. Then, the emergence of the attractive force from the pre-charged forces draws the

brane and the antibrane together. The combined brane-antibrane units go impartially to either side of the pre-expanding universe, resulting in the achiral brane-antibrane units. (Essentially, attractive force and repulsive force are the tools to form chirality and achirality.) Finally, pregravity and anti-pregravity emerge. In the universe, local interactions are either chirality-specific or achirality-specific. Unable to interact with the region inside the chiral pre-expanding universe, the achiral brane-antibrane units are separated from the chiral pre-expanding universe, and congregate in the area connecting the pre-universe and the pre-expanding universe. The result is the decrease of the connection between the pre-expanding universe and the pre-universe. However, as a non-localized global relation, $A = R + C$ continues with the right amount of C contributed by the pre-universe as long as there is still connection between the pre-universe and the pre-expanding universe.

As the pre-expanding universe grows with the chiral brane-antibrane units, the number of the achiral brane-antibrane units grows. Eventually, the pre-expanding universe is disconnected completely from the pre-universe by the achiral brane-antibrane units. Without C , the excess attractive force ($A > R$) between positive branes and negative charged antibranes causes the pre-expanding universe to collapse, and the repulsive force between pregravity and anti-pregravity causes the pre-expanding universe to invert. As the 9-brane and the 9-antibrane move toward each other, the 9-brane and the 9-antibrane turn inside, and pregravity and anti-pregravity turn outside. The "gulf" separating the pre-expanding universe and the pre-universe is formed. Eventually, the 9-brane and the 9-antibrane coalesce. At the end of the coalescence, the repulsion between pregravity and anti-pregravity causes a bounce after the collapse.

At this point, the complete coalescence leads to the loss of the properties of brane and antibrane in terms of the membrane property, the pre-charged force, the pre-strong force, and chirality. The result is the generation of the achiral mixed 9-particle with the multiple dimensional Kaluza-Klein structure without the requirements for identical space dimensions and a fixed number of space dimensions as in superstring. All forces formed previously become achiral. The bounce results in the mixed pre-expanding universe, consisting of four equal parts: two groups of achiral mixed 9-particles, achiral pregravity, and achiral anti-pregravity as Fig. 5.

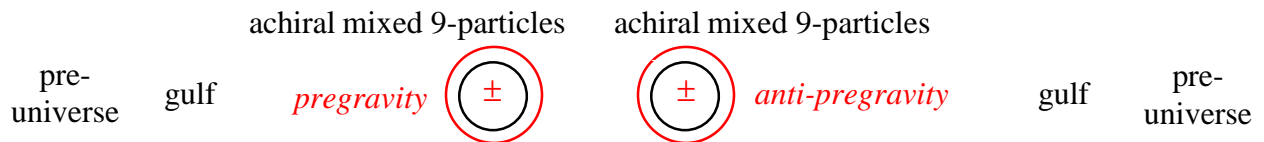


Fig. 5: the mixed pre-expanding universe

The interactions between branes in the form of collision are proposed in various brane models [6, 7, 8]. The cyclic universe model based on the ekpyrotic universe [9] has the collapse-singularity-bounce scheme.

The size of the pre-expanding universe is determined by the ratio between the number of the chiral units and the number of the achiral units. The pre-universe and the mixed pre-expanding universe are different in the composition of objects and vacuums, and

are separated from each other permanently. Consequently, the two universes are completely transparent to each other. Without relation with the pre-universe, the mixed pre-expanding universe has its own vacuum energy that decreases from the non-zero in the pre-universe to zero. With decreasing vacuum energy and the Kaluza-Klein structure without a fixed number of space dimensions, the space-time dimension and the mass dimension of mixed 9-particles decrease to lower dimensional space-time and lower dimensional mass. The decrease to lower mass dimension results in the fractionalization of mixed 9-particles into lower mass particles, leading to the expansion of the universe. The fractionalization leads to the cosmic expansion into the completely transparent pre-universe. It is the start of the expanding universe. To the pre-universe, the expanding universe is a missing region.

3. *The Expanding Universe: the Big Band and the Big Bang*

The cosmic expansion in terms of the fractionalization of 9-mixed particles involves two different modes for the two sides of the expanding universe: the big band mode for the hidden universe and the big bang mode for the observable universe as Fig. 6.

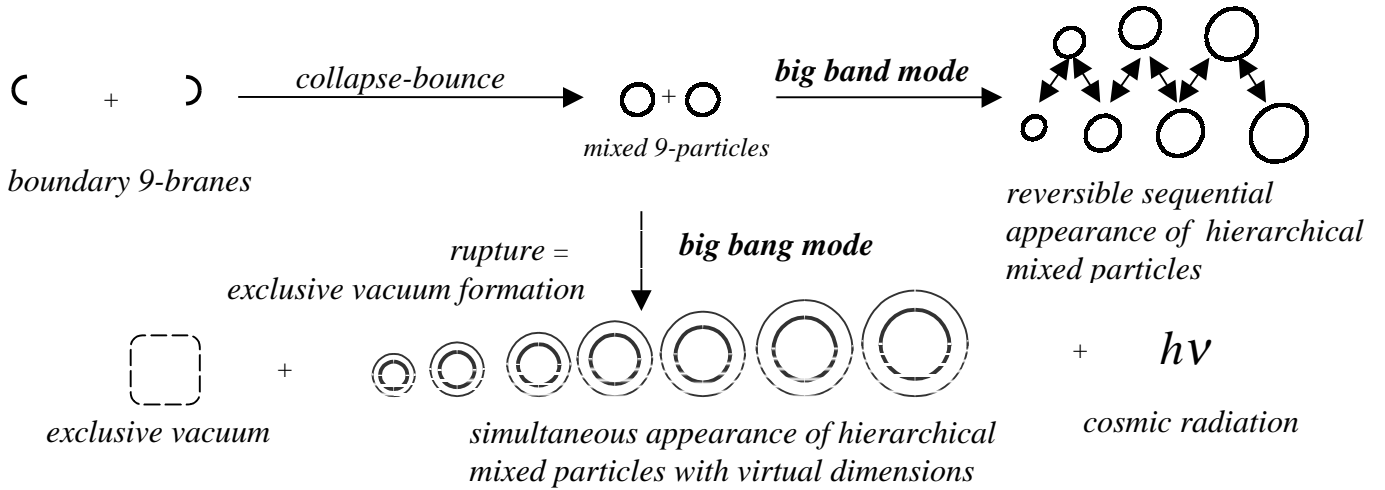


Fig. 6: the big band mode and the big bang mode

The big band mode is used in the hidden universe. In the big band mode, the vacuum energy decreases to zero gradually, the decrease in space-time dimension occurs simultaneously with the decrease in mass dimension sequentially. The decrease to lower mass dimension is through variable supersymmetry, which transforms a boson (or fermion) from one point to the boson (or fermion) with lower energy at another point at lower mass dimension. Thus, such variable supersymmetry results in the fractionalization of higher mass dimensional particles and the cosmic expansion at the same time. The result is the slow cosmic expansion with simultaneous decrease in space-time dimension and the mass dimension. The mixed 9-particles fractionalize into lower dimensional mixed particles from 8 to 3 ($9D$ to $4D$) sequentially, where p particle has $p + 1$ space-time dimension, D .

At the end of the cosmic expansion, the hidden universe undergoes slow condensation back to the mixed 10D particle with simultaneous increase in space-time dimension and mass dimension sequentially. The hidden universe undergoes expansion and contraction, like a big elastic rubber band (big band) as the top figure in Fig. 6.

The big bang mode is used in the observable universe. In the big bang mode, the vacuum energy decreases immediately to zero with 4D space-time, resulting in four-dimensional space-time generates 4D (four space-time dimensional) 10D (ten mass dimensional) particles with additional dimension for gravity. 10D particles immediately fractionalize into the mixture of particles from 4D to 10D. The mechanism for the immediate fractionalization is to differentiate mass dimensions in every 10D particle into real dimensions and virtual dimensions by exclusive vacuum. Real particles occupy real mass dimensions, and virtual particles occupy virtual dimensions. At the ground state, exclusive vacuum in virtual dimensions excludes real particles from virtual dimensions. At the high-energy level, real particle can expansion into virtual dimensions. For example, for the ground state of 4D particle (bayonic matter), the real particle with real mass occupies the first four mass dimensions, and exclusive vacuum exclude the real particle from fifth to tenth mass dimensions plus dimension for gravity. In the same way, 5D particle occupies the first five mass dimensions. Different real particles occupy different real dimensions, resulting in immediate fractionalization into the mixture of particles from 4D to 10D. The total mass of the universe is divided into seven equal portions for the seven types of particles as shown in the bottom figure in Fig. 6.

Exclusive vacuum is derived from the dislocation of mass from 10D particle. In the CP symmetry, equal and opposite positive and negative charges for the two internal boundary branes within the mixed particle as 10D particle results in the dislocation of energy by the internal annihilation (implosion). The empty space left behind the dislocation is exclusive vacuum, and the dislocated energy is cosmic radiation. Cosmic radiation is forced to travel by permanent exclusion of its own space: exclusive vacuum. The 10D particles with CP asymmetry remain as 10D particles.

10D particles absorb exclusive vacuum from cosmic radiation to generate immediate fractionalization. The resulting mixture of particles from 4D to 10D has larger size than pure 10D particles, so the fractionalization involves a cosmic expansion. The mechanism for such expansion involves 10D particles as negative pressure as in the inflation theory [10]. In the equation for the acceleration, $\frac{\ddot{a}}{a} = -\frac{4\pi}{3m_{PL}^2}(\rho + 3p)$, the

negative pressure ($\rho + 3p < 0$) leads to $\ddot{a} > 0$, resulting in inflation. High-energy 10D particles absorb exclusive vacuum exponentially, resulting in exponential inflation. At the beginning of the inflation, inflationary cosmic radiation (ϕ) has high potential ($V(\phi)$). At the end, all potential is converted into ϕ and exclusive vacuum that induces the immediate fractionalization.

During the inflation, due to the negative pressure from 10D particles, cosmic radiation is not free to travel. Thus, at the end of the inflation, the size of the universe is exactly equal to the sum of spaces allowed for the particles from 4D to 10D, held together by gravity. After the inflation, the absence of the negative pressure allows cosmic radiation

to travel freely within the domain of gravity. Free traveling cosmic radiation allows the universe to cool by the non-inflationary decelerating expansion. In summary, the cosmic expansion for the observable universe consists of the inflationary expansion for the immediate fractionalization and the non-inflationary expansion for thermal cooling.

The mixed particles that are not annihilated have asymmetrical charge-parity (CP asymmetry), in such way that the mixed particle has two asymmetrical sets (main and auxiliary) of mass dimensions from the two boundary branes within the mixed particle. The auxiliary set is dependent on the main set, so the mixed particle appears to have only one set of space dimensions. Since there are real and virtual mass dimensions for every particle, there are main real, auxiliary real, main virtual, auxiliary virtual mass dimensions. Thus, for the four-mass-dimensional particle (baryonic matter), there are 4D main real, 4D auxiliary real, 7D main virtual, and 7D auxiliary virtual mass dimensions. These mass dimensions are for the mixture of leptons and quarks, and form the base for the periodic table of elementary particles [3].

The summary of the cosmic evolution is described in Fig. 7.

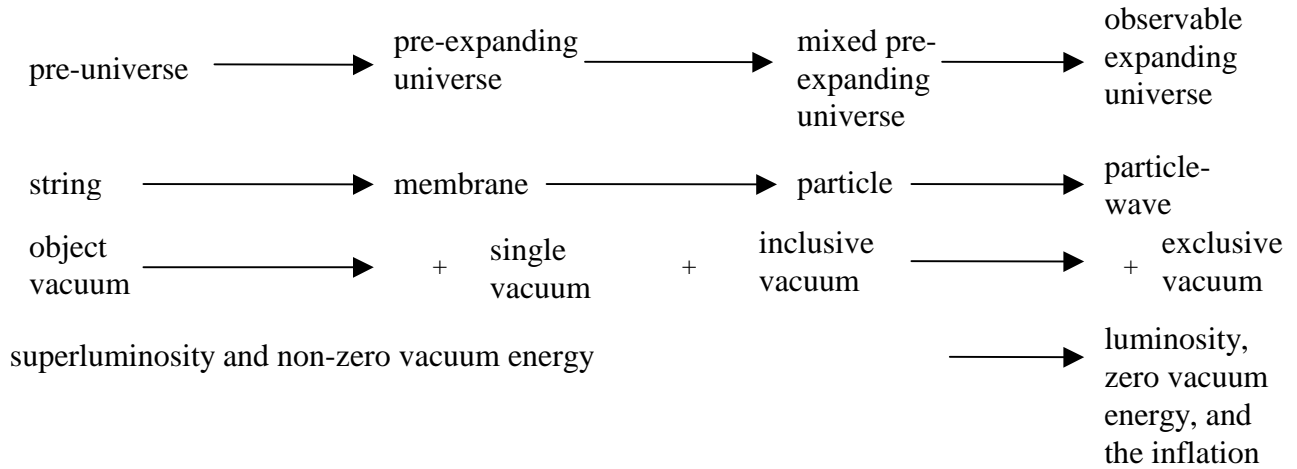


Fig. 7: the cosmic evolution

The hidden universe and the observable universe are incompatible in dimensionality and in physical laws (with and without exclusive vacuum), so they are completely transparent to each other until they are compatible in dimensionality. This two-universe model appears also in the two-universe (visible and hidden) model in the cyclic ekpyrotic universe model [9].

4. *The Formation of Inhomogeneous Structure*

The observable universe consists of baryonic matter and dark matter. The baryonic matter has the 4-dimensional mass. Dark matter consists of six types of particles with mass dimensions from 5D to 10D. Both dark matter and baryonic matter share the same long-ranged gravity. Dark matter does not have electromagnetism [3], so it cannot be seen, but it can be observed by gravity. Such difference in electromagnetism results in the mass

dimensional incompatibility between baryonic matter and dark matter. There are seven types of particles from 4D to 10D. Baryonic matter is one of the seven types of particles at equal mass proportions, so the baryonic mass fraction is $1/7$ (0.14). The universal baryonic mass fraction was found to be 0.13 by the observations of primordial deuterium abundance [11]. The calculated value agrees well with the observed value.

The Inflationary Universe scenario [10] provides possible solutions of the horizon, flatness and formation of structure problems. In the standard inflation theory, quantum fluctuations during the inflation are stretched exponentially so that they can become the seeds for the formation of inhomogeneous structure such as galaxies and galaxy clusters. They also produce anisotropies in CMB (cosmic microwave background). However, without fine-tuning, the calculated amplitude of the density perturbation induced by quantum fluctuations during the inflation is much larger than the observed amplitude in CMB. The small density perturbation is a serious problem in the inflation theory [12].

The universe is supposed to be largely composed of cold dark matter. The density of dark matter is supposed to be the highest (cusp) in the middle of galaxy, but the cusp has not been definitely confirmed by observation [13]. The cusp problem is a serious problem in the theory of dark matter.

In the cosmic evolution, quantum mechanics is fully developed only after the inflation. The inflation does not involve quantum fluctuation, so instead of quantum fluctuations, the incompatibility between ordinary matter and dark matter due to the difference in electromagnetism brings about the formation of inhomogeneous structure. It is analogous to the formation of emulsion (milk) by the incompatibility between two materials such as oil and water. (The incompatibility between oil and water is due to electromagnetic property in terms of polarity.) Such incompatible dark matter (IDM) does not stay permanently in the middle of baryonic matter. Therefore, IDM avoids both the small density perturbation problem and the cusp problem. Incompatible dark matter precludes detecting dark matter on the earth made by baryonic matter.

Cosmic radiation is compatible with both baryonic matter and dark matter through the commonality in exclusive vacuum. The incompatibility between baryonic matter and dark matter increases linearly with decreasing temperature of cosmic radiation whose temperature decreases with increasing size of the universe. Thus, the incompatibility increases with increasing size of the universe. The whole universe behaves as one unit of emulsion. The mass ratio between baryonic matter and dark matter is 1 to 6. As water domains surround oil droplets (the smaller part) in emulsion, dark matter domains surrounded baryonic droplets (the smaller part). These dark matter domains later became the dark matter halos, and the baryonic droplets became galaxies, clusters, and superclusters.

Incompatible materials separate from each other. The force to maintain the separation is the anti-expansion force to keep one material to expand into the region of other material. The dimensional incompatibility between the baryonic droplet and the dark matter halo is expressed as the interfacial zone between the two different matter domains as Fig. 8.

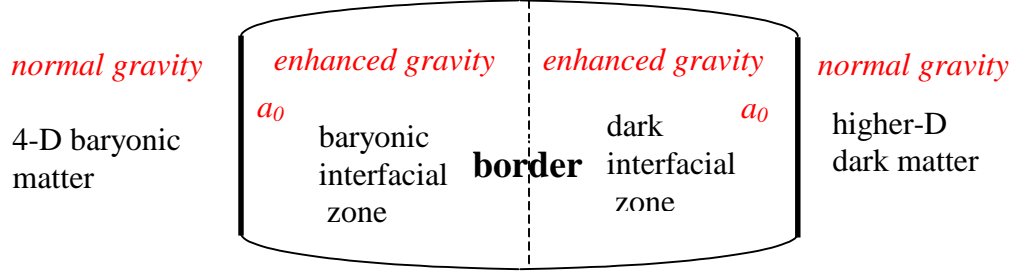


Fig. 8: the anti-expansion force in the interfacial zone between baryonic matter and dark matter. The region with the acceleration higher than a_0 has normal gravity, and the interfacial zone with the acceleration lower than a_0 has the enhanced gravity.

The baryon-dark border between baryonic matter and dark matter is in the middle of the interfacial zone. The interfacial zone consists of the dark interfacial zone and the baryonic matter zone for two sides of the baryon-dark border. The force in the interfacial zone is the anti-expansion force as the enhancement of gravity in the interfacial zone away from the baryon-dark border to maintain a clear border. Such enhancement of gravity is same as the enhancement of gravity in the M. Milgrom's [1] Modified Newtonian Dynamics (MOND).

The starting line of the interfacial zone has a_0 as the acceleration. The Newtonian acceleration is a_N . In the interfacial zone, $a_N < a_0$. The effective acceleration a_b for the baryonic interfacial zone and the a_d for the dark interfacial zone are as follows.

$$\begin{aligned} a_b &= (a_N a_0)^{1/2} \\ a_d &= (a_N a_0)^{1/2} \end{aligned} \quad (6)$$

$$\text{enhancement of gravity away from the border} \propto (a_0 - a_N)^{1/2} \quad (7)$$

In the equilibrium state, a_b is symmetrical to a_d . At a distance, r , away from the border,

$$\begin{aligned} a_{b,r} &= a_{d,r} \\ (a_0 - a_N)_{b,r}^{1/2} &= (a_0 - a_N)_{d,r}^{1/2} \end{aligned} \quad (8)$$

The enhancement of gravity away from the border in the baryonic interfacial zone results in flat rotation curves as observed in some galaxies [14]. The enhancements of gravity away from the border in both interfacial zones are equal and cancel each other. The net anti-expansion force is zero. This cancellation of the enhancement of gravity is the global cancellation of the deviation (the anti-expansion force) between MOND and Newtonian gravity in a large area that is larger than the interfacial zones. The distance from the center of baryonic mass to the starting line of the interfacial zone increases with increasing a_0 . The size of the universe is directly proportional to a_0 .

As in emulsion, the size of the baryonic droplet grows with increasing incompatibility between dark matter and baryonic matter. As the incompatibility between dark matter and baryonic matter increases with increasing size of the universe, the droplet develops the droplet growth potential as the potential to increase the mass of the droplet. The droplet growth potential converts to the non-zero net anti-expansion force by moving the baryon-dark border outward to absorb free baryonic matter outside and to merge with other droplets. Such movement of the baryon-dark border is derived from the uneven enhancement of gravity in the interfacial zone: high enhancement of gravity away from the border in the dark interfacial zone and low or no enhancement of gravity away from the border in the baryonic interfacial zone.

$$\begin{aligned} a_{b,r} &< a_{d,r} \\ (a_0 - a_N)_{b,r}^{1/2} &< (a_0 - a_N)_{d,r}^{1/2} \end{aligned} \quad (9)$$

In the extreme case, $a_b = a_N$, so there is low or no enhancement of gravity in the baryonic interfacial zone as observed as falling rotation curves in bright galaxies [14].

In the case of the trapping of free dark matter inside the baryonic droplet, the incompatibility between dark matter and baryonic matter generates the droplet contraction potential. The potential is to contract the droplet in order to remove the free dark matter inside. The droplet contraction potential converts to the non-zero net anti-expansion force by moving the baryon-dark border inward to expel free dark matter inside. The inward movement involves the uneven enhancement of gravity: low enhancement of gravity in the dark interfacial zone and high enhancement of gravity in the baryonic interfacial zone.

$$\begin{aligned} a_{b,r} &> a_{d,r} \\ (a_0 - a_N)_{b,r}^{1/2} &> (a_0 - a_N)_{d,r}^{1/2} \end{aligned} \quad (10)$$

The high enhancement of gravity away from the border in the baryonic interfacial zone is observed as rising rotation curves in dwarfs and low surface brightness galaxies [14].

In emulsion, oil exists as free oil among water or as oil in oil droplet. Similarly, baryonic matter exists as free baryonic matter among dark matter or as baryonic matter in the baryonic droplet. At the beginning of the expanding universe with high cosmic radiation temperature, baryonic matter and dark matter were completely compatible with each other, and baryonic matter existed entirely as free baryonic matter. As the size of the universe increased, the size of the baryonic droplets increased with the increasing incompatibility between baryonic matter and dark matter. At the time of recombination (neutralization), the baryonic matter in the small baryonic droplets coexisted with free baryonic matter in the surrounding. With electromagnetic attraction, the baryonic droplet had higher matter density than the surrounding dark matter without electromagnetism and isolated free baryonic matter. The density difference between the baryon matter in the baryonic droplet and the baryonic matter in the surrounding led to anisotropies observed in the CMB.

When the CMB occurred moment before the recombination, because of radiation pressure, the density in the baryonic droplet was much lower than the normal density

without radiation pressure. After the decoupling between baryonic matter and radiation at the recombination, the absence of radiation pressure allowed the density of the droplet to return to the normal density quickly.

As the universe expanded, the increasing incompatibility drove increasing amount of free baryonic matter into the baryonic droplets. The growth of the baryonic droplet by the increasing incompatibility from the cosmic expansion coincided with the growth of the baryonic droplet by gravitational instability from the cosmic expansion. The pre-galactic universe consisted of the growing baryonic droplets surrounded by the dark matter halos, which connected among one another in the form of filaments and voids.

5. *The Evolution of Galaxies, Clusters, and Superclusters*

When there were many baryonic droplets, the merger among the baryonic droplets became another mechanism to increase the droplet size and mass. In Fig. 9, the baryonic droplets (A and B) merged into one droplet (C). When three or more droplets merged together, dark matter was likely trapped in the merged droplet (D, E, and F in Fig. 9). The droplet with trapped dark matter inside is the heterogeneous baryonic droplet, while the droplet without trapped dark matter inside is the homogeneous baryonic droplet.

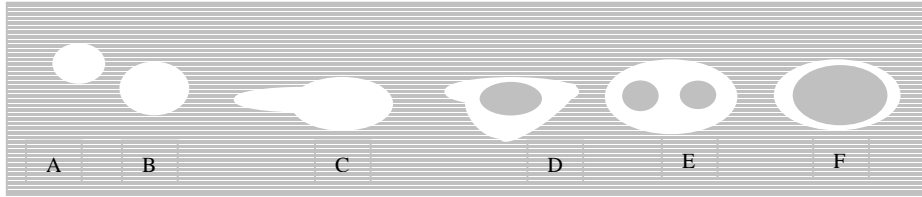


Fig. 9: the homogeneous baryonic droplets (A, B, and C), and the heterogeneous baryonic droplets (D, E, and F)

For the heterogeneous droplet, the dark matter core is essentially the dark droplet surrounded by the baryonic matter shell. As the dark droplet, the dark matter core has the droplet growth potential proportional to the size of the universe, and has the baryon-dark border moving toward the baryonic matter shell. Thus, two baryon-dark borders in the heterogeneous droplet are the external border between the dark matter halo and the and the dark matter halo and the internal baryon-dark border between the baryonic matter shell and the dark matter core. The external border moved toward the dark matter halo, while the internal border moved toward the baryonic matter shell. When a section of the internal border and a section of the external border merged, the dark matter from the dark matter core moved to the dark matter halo away from the heterogeneous droplet, and the droplet became homogeneous.

When the temperature dropped to $\sim 1000^{\circ}\text{K}$, some hydrogen atoms in the droplet paired up to create molecular baryonic matter. The most likely place to form such molecular baryonic matter was in the interior part of the droplet. For heterogeneous droplet, molecular baryonic matter formed a molecular layer around the core. Molecular

hydrogen cooled the molecular layer by emitting infrared radiation after collision with atomic hydrogen. Eventually, the temperature of the molecular layer dropped to around 200 to 300°K, reducing the gas pressure and allowing the molecular layer to continue contracting into gravitationally bound dense molecular layer with high viscosity.

Without electromagnetism, the viscosity of dark matter remained low. The viscosity in the dense molecular layer around the core slowed the movement of the internal baryon-dark border toward the baryonic matter shell. On the other hand, the low-viscosity dark matter did not hinder the movement of the external baryon-dark border toward the dark matter halo. The increasing difference in the speeds of movement between the internal and external borders increased the fraction of the heterogeneous baryonic droplets.

Subsequently, the whole baryonic matter shell became the dense molecular layer. The dense baryonic matter shell contracted into gravitationally bound clumps, which prevented the movement of the internal border. The dark matter cores build up the internal pressure from the accumulated droplet growth potential. Eventually, the core with high internal pressure caused the eruption to the droplet. The dark matter rushed out of the droplet within a short time, and the baryonic matter shell collapsed. This eruption is much larger in area and much weaker in intensity than supernova. The “big eruption” of the baryonic droplet brings about the morphologies of galaxies.

If there was very small or no dark matter core as in the homogeneous baryonic droplet, the shape of the resulting galaxy is circular as in the E₀ type elliptical galaxy. If the relative size of the dark matter core was small, the change in the shape of the shell was minor. It is like squeezing out orange juice (dark matter core) through one opening on the orange skin (baryonic matter shell). As the dark matter core moved out, the baryonic matter shell stretched in the opposite direction. The minor change resulted in an elliptical shape as in E₁ to E₇ elliptical galaxies, whose lengths of major axes are proportional to the relative sizes of the dark matter core.

During the collapse of the baryonic matter shell in the big eruption, the collision produced a shock front of high density, which resulted in the formation of many massive first stars. After few million years, such massive first stars became supernovas and black holes. Most of the massive first stars became black holes without contributing to the metal enrichment of the surrounding. The mergers of black holes generated the supermassive black hole as the nucleus of quasar. Such first quasar galaxies that occurred as early as $z = 6.28$ were observed to have about the same sizes as the Milky Way [15].

The supernova shock wave induced the formation of stars in the exterior part of the droplet. The time difference in the formations of the nucleus and the formation of stars in the surface was not large, so there are small numbers of observed young stars in elliptical galaxies. This formation of galaxy follows the monolithic collapse model [16], in which baryonic gas in galaxies collapses to form stars within a very short period. Elliptical galaxies continue to grow slowly as the universe expands.

If the size of the dark matter core is medium (D in Fig. 9), it involves a large change on the baryonic matter shell. It is like to release air (the dark matter core) from a balloon (the baryonic matter shell) filled with air. As the dark matter core moved out, the baryonic matter shell moved in the opposite direction.

If there was only one opening as an air balloon with one opening, the dark matter stream from the dark matter core and the baryonic stream from the baryonic matter shell moved in opposite directions. Later, the two streams separated. The dark matter stream merges with the surrounding dark matter. The baryonic stream with high momentum penetrated the surrounding dark matter halo. As the baryonic stream penetrated into the dark matter halo, it met resistance from the anti-expansion force. Eventually, the stream stopped.

The minimization of the interfacial area due to the incomparability between baryonic matter and dark matter transformed the shape of the stream from linear to disk. (The minimization of the interfacial area is shown in the water bead formation on a wax paper.) To transform into disk shape, the stream underwent differential rotation with the increasing angular speeds toward the center. The fast angular speed around the center allowed the winding of the stream around the center. After few rotations, the structure consisted of a bungle was formed by wrapping the stream at the center and the attached spiral arms as spiral galaxy as Fig. 10.

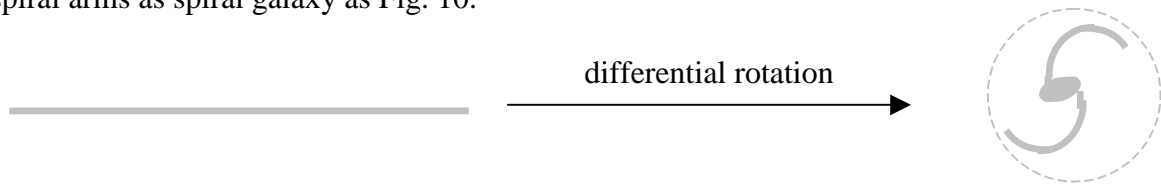


Fig. 10: from the linear baryonic stream to normal spiral galaxy with the baryon-dark border (dot line)

During the stream formation, the high-density region derived from the collision during the collapse spread out, so the density of the stream was too low to form stars. As the stream wrapped around at the center, the wrapping of the stream produces the high-density region for the star formation in a steady pace. Thus, the first stars and the black holes at the center in spiral galaxies are smaller than in elliptical galaxies. The stars at the center became black holes and supernovas that induced the star formation in spiral arms. The massive center area decreases the angular speed around the center, greatly retarding the winding of the spiral arms around the center. With this steady pace for the star formation, there are still many young stars in spiral galaxies. When there were more than one baryonic stream in the same general direction, there are more than two spiral arms.

Some streams went through the dark matter halos, and entered into the adjacent baryonic droplets. The adjacent droplet captured a part of the stream, and another part of the stream continued to move to the dark matter halo, and finally settled near the droplet in the dark matter halo. Dependent on the direction of the entry, the captured part of the stream later became a part of the disk of the host galaxy, star clusters in the halo, or both. The part of the stream that settled near the droplet became the dwarf spheroidal galaxy. Under continuous disruption and absorption of the tidal interaction from the large galaxy nearby, the dwarf spheroidal galaxy does not have well-defined baryonic-dark border, disk, and internal rotation.

When two connected dark matter cores inside far apart from each other (E in Fig. 9) generated two openings in opposite sides of the droplet, the momentum from the two

opposite dark matter streams canceled each other nearly completely. The result was the slow moving baryonic droplet. Two opposite baryonic streams formed side by side with the two opposite dark matter streams. When the baryonic stream entered the dark matter halo, the size of the stream decreased due to the anti-expansion force by the dark matter, so there were the thick stream in the baryonic matter shell and the thin stream in the dark matter halo. As the baryonic stream penetrated into the dark matter halo, it met resistance from the anti-expansion force. Eventually, the stream stopped. The result after few differential rotations is the structure with one center, one bar from the thick stream stranding across the center, and arms attached to the bar as bar spiral galaxy as Fig. 11.

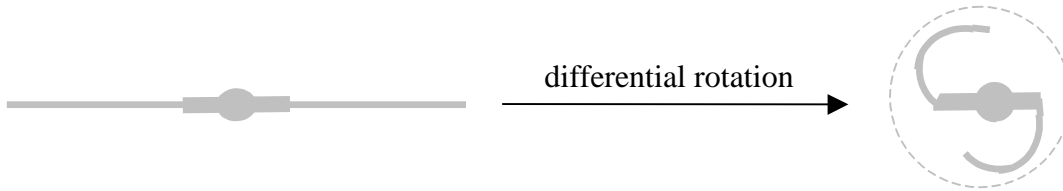


Fig. 11: from the barred linear baryonic stream to barred spiral galaxy with the baryon-dark border (dot line)

The result is barred spiral galaxy. As in normal spiral galaxy, the length of the spiral arm depends on the size of the dark matter core. The smallest dark matter core for barred spiral galaxy brings about SBa, and the largest dark matter core brings about SBd. The stars form in the low-density spiral arms much later than in the nucleus, so they are many young stars in the spiral arms.

If the size of the dark matter core was large (F in Fig. 9), the total dark matter mass was nearly large enough or large enough for dark matter to have low droplet growth potential. The escape of the dark matter from the droplet involved little or no eruption, resulting in the gradual migration of large amount of dark matter outward and the gradual migration of small amount of baryonic matter inward. Such opposite migrations are long and continuous processes. The result is irregular galaxy. When enough baryonic matter migrated to the center, and first star formation started. As baryonic matter continues migrating toward the center, the star formation continues in a slow rate up to the present time.

At the end of the big eruption, vast majority of baryonic matter was primordial free baryonic matter resided in dark matter outside of the galaxies from the big eruption. This free baryonic matter constituted the intergalactic medium (IGM). Stellar winds, supernova winds, and quasars provide heat and heavy elements to the IGM as ionized baryonic atoms. The heat prevented the formation of the baryonic droplet in the IGM.

Galaxies merged into new large galaxies, such as giant elliptical galaxy and cD galaxy ($z > 1-2$). Similar to the transient molecular cloud formation from the ISM (interstellar medium) through turbulence, the tidal debris and turbulence from the mergers generated the numerous transient molecular regions, which located in a broad area [17]. The incompatibility between dark matter and baryonic matter transformed these transient molecular regions into the stable second-generation baryonic droplets surrounded by the

dark matter halos. The baryonic droplets had much higher fraction of hydrogen molecules, much lower fraction of dark matter, higher density, and lower temperature, and lower entropy than the surrounding. The baryonic droplets started small with the enormous droplet growth potential. The rapid growth of the baryonic droplets drew large amount of the surrounding IGM inward, generating the IGM flow shown as the cooling flow. The IGM flow induced the galaxy flow. The IGM flow and the galaxy flow moved toward the merged galaxies, resulting in the protocluster ($z \sim 0.5$) with the merged galaxies as the cluster center.

Before the protocluster stage, spirals grew normally and passively by absorbing gas from the IGM as the universe expanded. During the protocluster stage ($z \sim 0.5$), the massive IGM flow injected a large amount of gas into the spirals that joined in the galaxy flow. Most of the injected hot gas passed through the spiral arms and settled in the bungle parts of the spirals. Such surges of gas absorption from the IGM flow resulted in major starbursts ($z \sim 0.4$) [18]. Meanwhile, the nearby baryonic droplets continued to draw the IGM, and the IGM flow and the galaxy flow continued. The results were the formation of high-density region, where the galaxies and the baryonic droplets competed for the IGM as the gas reservoir. Eventually, the maturity of the baryonic droplets caused a decrease in drawing the IGM inward, resulting in the slow IGM flow. Subsequently, the depleted gas reservoir could not support the major starbursts ($z \sim 0.3$). The galaxy harassment and the mergers in this high-density region disrupted the spiral arms of spirals, resulting in S0 galaxies with indistinct spiral arms ($z \sim 0.1 - 0.25$). The transformation process of spirals into S0 galaxies started at the core first, and moved to the outside of the core. Thus, the fraction of spirals decreases with decreasing distance from the cluster center [18].

The static and slow-moving second-generation baryonic droplets turned into dwarf elliptical galaxies and globular clusters. The fast moving second-generation baryonic droplets formed the second-generation baryonic stream, which underwent a differential rotation to minimize the interfacial area between the dark matter and baryonic matter. The result is the formation of blue compact dwarf galaxies (BCD), such as NGC 2915 with very extended spiral arms. Since the star formation is steady and slow, so the stars formed in BCD are new.

The galaxies formed during $z < 0.1-0.2$ are mostly metal-rich tidal dwarf galaxies (TDG) from tidal tails torn out from interacting galaxies. In some cases, the tidal tail and the baryonic droplet merge to generate the starbursts with higher fraction of molecule than the TDG formed by tidal tail alone [19].

When the interactions among large galaxies were mild, the mild turbulence caused the formation of few molecular regions, which located in narrow area close to the large galaxies [17]. Such few molecular regions resulted in few baryonic droplets, producing weak IGM flow and galaxy flow. The result is the formation of galaxy group, such as the Local Group, which has fewer dwarf galaxies and lower density environment than cluster.

Clusters merged to generate tidal debris and turbulence, producing the baryonic droplets, the ICM (intra-cluster medium) flow, and the cluster flow. The ICM flow and the cluster flow directed toward the merger areas among clusters and particularly the rich clusters with high numbers of galaxies. The ICM flow is shown as the warm filaments outside of cluster [20]. The dominant structural elements in superclusters are single or

multi-branching filaments [21]. The cluster flow is shown by the tendency of the major axes of clusters to point toward neighboring clusters [22]. Eventually at the maximum incompatibility between dark matter and baryonic matter, the observable expanding universe will consist of giant voids and superclusters surrounded by the dark matter halos.

In summary, the whole observable expanding universe is the “Milky Universe” as one unit of emulsion with increasing incompatibility between dark matter and baryonic matter. The five periods of baryonic structure development are the free baryonic matter, the baryonic droplet, the galaxy, cluster, and the supercluster periods as Fig. 12. The first-generation galaxies are elliptical, normal spiral, barred spiral, irregular, and dwarf spheroidal galaxies. The second-generation galaxies are giant ellipticals, cD, evolved S0, dwarf ellipticals, BCD, and TDG. The universe now is in the early part of the supercluster period.

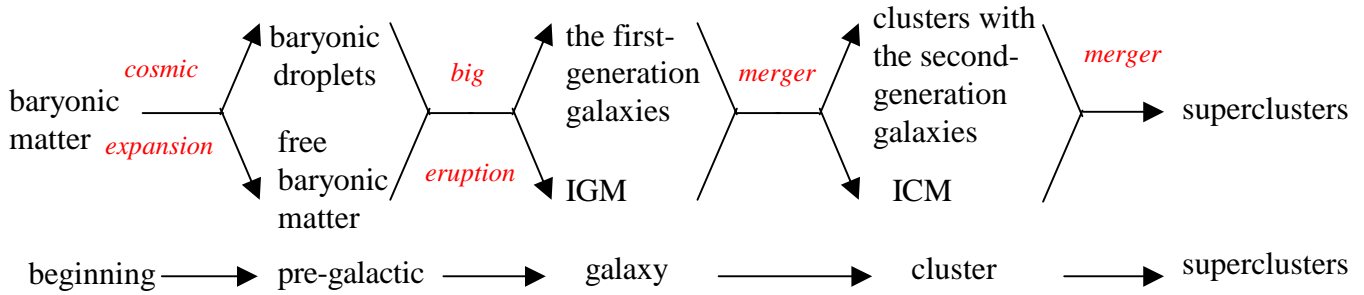


Fig. 12: the five levels of baryonic structure in the Milky Universe

6. Conclusion

The variable speed of light is quantized by variable space-time dimension, resulting in variable mass in terms of variable mass dimension. The transformation of variable mass in terms of variable mass dimension is by variable supersymmetry, relating to dimensional fermions and bosons.

The evolution of our expanding universe involves four stages: the pre-universe, the pre-expanding universe, the mixed pre-expanding universe, and the expanding universe. The evolution involves the evolution of objects-vacuums, which consist of four objects (string, membrane, particle, and particle-wave) and four vacuums (object vacuum, single vacuum, inclusive vacuum, and exclusive vacuum). In the pre-universe, object and vacuum take turn to exist equally at the same location. It is an equilibrium state between vacuum and the pair of ten-dimensional superstring and anti-superstring with a non-zero vacuum energy. The vacuum fluctuation (Figs. 1, 2, 3, and 4) results in the pre-expanding universe with the chiral boundary positive charged 9-brane and the chiral boundary negative charged 9-antibrane separated by pregravity (the predecessor of gravity) and anti-pregravity. The collapse and the bounce of the pre-expanding universe result in the generation of the achiral mixed 9-particle with the multiple dimensional Kaluza-Klein structure, achiral pregravity, achiral anti-pregravity, and zero vacuum energy (Fig. 5).

The decrease in vacuum energy leads to the fractionalization of mixed 9-particles into mixed particles with lower space-time and mass dimensions, resulting in the cosmic expansion. The two modes, the big band and the big bang, of the cosmic expansion lead to two universes, the hidden universe and the observable universe, respectively as shown in Fig. 6. In the big band mode, the space-time and mass dimensions decrease and then increase gradually and sequentially. In the big bang mode, the space-time dimension decreases to four immediately, and the fractionalization of mixed 9-particles completes immediately. The emergence of exclusive vacuum leads to the immediate fractionalization and the inflation that brings about the big bang, cosmic radiation, elementary particles, dark matter, entropy, force fields, and quantum mechanics. The cosmic evolution involving objects and vacuums is shown in Fig. 7.

The observable universe is the Milky Universe. In the Milky Universe model, baryonic matter with four-mass dimension is incompatible with dark matter with higher mass-dimensions. Both of them are compatible with cosmic radiation through exclusive vacuum. The incompatibility increases with the increasing size of the universe. Such incompatibility brings about the formation of inhomogeneous structure (anisotropies in the CMB) where the baryonic matter domains surrounded by the dark matter halos as oil droplets surrounded by water in emulsion. The gravitational interaction between baryonic matter and dark matter can be described by the Modified Newtonian Dynamics (MOND) (Fig. 8). The five periods (Fig. 12) of baryonic structure development in the order of increasing incompatibility between baryonic matter and dark matter are the free baryonic matter, the baryonic droplet, the galaxy, the cluster, and the supercluster periods. The transition to the baryonic droplet generates density perturbation in the CMB. The transition from the baryonic droplet to galaxy is through the big eruption for the formations of the first-generation galaxies, including elliptical, normal spiral (Fig. 10), barred spiral (Fig. 11), irregular, and dwarf spheroidal galaxies. The transitions to cluster and supercluster are the mergers and interactions of galaxies for the formation of the second-generation galaxies, including modified giant ellipticals, cD, evolved S0, dwarf elliptical, BCD, and tidal dwarf galaxies. The universe now is in the early part of the supercluster period. The whole observable expanding universe behaves as one unit of emulsion with increasing incompatibility between dark matter and baryonic matter.

In conclusion, the new MOND with incompatible dark matter has its origin in cosmology based on superstring. It explains in details the evolution of galaxies.

References

* chung@wayne.edu

- [1] M. Milgrom, astro-ph/0207231, astro-ph/0112069; R. H. Sanders and S. McGaugh astro-ph/0204521
- [2] G. Amelino-Camelia, Int. J. Mod. Phys. D11 (2002) 35 [gr-qc/0012051]; Phys. Letts. B510 (2001) 255 [hep-th/0012238]; S. Alexander and J. Magueijo, hep-th/0104093;

- J. Magueijo and L. Smolin, Phys. Rev. Lett. 88 (2002) 190403; J. Magueijo, “Faster Than the Speed of Light: The Story of a Scientific Speculation” Perseus, 2003
- [3] D. Chung, hep-th/0111147, hep-th/0201115
 - [4] L. Randall and R. Sundrum, Nucl. Phys. **B557** (1999) 79; Phys. Rev. Lett. **83** (1999) 3370 ; Phys. Rev. Lett. **83** (1999) 4690
 - [5] P. Horava and E. Witten, Nucl. Phys. **B475** (1996) 94 [hep-th/9603142].
 - [6] J. Khoury, B. A. Ovrut, P. J. Steinhardt, and N. Turok, hep-th/0103239; R. Kallosh, L. Kofman, and A. Linde, hep-th/0104073; S. Rasanen, hep-th/0111279.
 - [7] G. Dvali, Q. Shafi, and S. Solganik, hep-th/0105203; C. P. Burgess, M. Majumdar, D. Nolte, F. Quevedo, G. Rajesh, and R. J. Zhang, hep-th/0105204.
 - [8] M. Bucher, hep-th/0107148; A. Nornov, hep-th/0109090; M.F. Parry, D. A. Steer, hep-th/0109207, D. Langlois, K. Maeda, D. Wards, gr-qc/0111013; J. Garriga, T. Tanaka, hep-th/0112028, S. Mukherji and M. Peloso, hep-th/0205180, P. Brax and D. A. Steer, hep-th/0207280, Y. S. Myung, hep-th/0208086
 - [9] J. Khoury, B. A. Ovrut, N. Seiberg, P. J. Steinhardt, and N. Turok, hep-th/0108187; P. J. Steinhardt, and N. Turok, hep-th/0111098; P. J. Steinhardt, and N. Turok, astro-ph/0112537; J. Martin, P. Peter, N. Pinto-Neto, and D. Schwarz, hep-th/0112128; P. Steinhardt and N. Turok, astro-ph/0204479, R. Dave, R. R. Caldwell, P. J. Steinhardt, astro-ph/0206372
 - [10] A. H. Guth, Phys. Rev. D **23**, 347 (1981)
 - [11] D. Tytler, S. Burles, L. Lu, X-M, Fan, A. Wolfe, and B. Savage, AJ, **117** (1999) 63; F. C. van den Bosch, A. Burkert, and R. A. Swaters, astro-ph/0105082
 - [12] R. H. Bradenberger, astro-ph/0208103
 - [13] B. Moore, Nature 370 (1994) 629
 - [14] F. Combes, astro-ph/0206126
 - [15] R. Barkana and A. Loeb, astro-ph/0209515
 - [16] B. M. Tinsley and J. E. Gunn ApJ 203 (1976) 52
 - [17] C. Conselice, astro-ph/0212219
 - [18] B. M. Poggianti, astro-ph/0210233, S. F. Helsdon and T. J. Ponman, astro-ph/0212047
 - [19] S. Leon, J. Braine, P. Duc, V. Charmandaris, and E. Brinks, astro-ph/0208494, astro-ph/0210014
 - [20] M. Bonamente, M. Joy, and R. Liu, astro-ph/0211439
 - [21] J. Einasto, G. Hutsi, M. Einasto, E. Saar, D. L. Tucher, V. Muller, P. Heinamaki, and S. S. Allam, astro-ph/0212312
 - [22] M. J. West, astro-ph/9709289